

On the Interpretation of the Doppler Spectra of Ionospherically Propagated Ground Backscatter Echoes

J. A. Bennett

A.T.C. Research Laboratories, 59 Little Collins Street, Melbourne, Vic. 3000.

Abstract

The mechanism giving rise to the backscatter Doppler spectrum is discussed by means of a simple model. Attention is focused on the effect of movement of the region contributing to the echo which arises from time changes in the group velocity within the ionosphere. It is shown that the influence of these changes on the spectrum can be separated into two parts: (1) A change in the maximum possible width of the spectrum as a result of the change of the time for which an individual scatterer is contributing to the echo; this effect is independent of the scatterer distribution. (2) A possible narrowing of the spectrum as a result of the way in which the signals from individual scatterers combine; this effect depends upon scatterer distribution. Scatter from a fixed scattering surface and from dispersive waves (e.g. sea waves) is considered. A tentative extrapolation of the results to a more realistic model suggests that neither effect is likely to be significant in practical high-frequency radio experiments (except at short ranges with highly directional antennas), although they may be significant in acoustic wave simulations of the radio case.

Introduction

The spectral characteristics of ionospherically propagated ground backscatter echos are potentially capable of yielding information about rates of change in remote regions of the Earth's ionosphere and the surface of the sea (Crombie 1955; Croft 1972; Earl and Bourne 1975). If this potential is to be realized, the mechanism giving rise to the spectral characteristics must be understood. High frequency ionospheric scatter poses problems that do not arise in most radar systems because the ionosphere is both refractive and dispersive to radio waves as well as being time varying. Time changes in the refractive index of the ionosphere can give rise to Doppler frequency shifts (Bennett 1967, 1968), while time changes in the group refractive index can cause the region of space, that contributes to the echo at a fixed delay, to move with time. It is this second effect that we are particularly concerned with here. The influence of such movement on the time-average instantaneous frequency has been discussed at some length in recent years (Edwards and Thome 1962; Barry and Widess 1962; Agy 1969; Croft 1969, 1972) and it has been suggested that the effect depends critically on the nature of the scatterer. In many experiments the instantaneous frequency is not measured and, instead, a spectral analysis is performed on the echo. If a single frequency is chosen to characterize the echo spectrum, the best choice is probably the mean frequency of the power spectrum, although this is not in general equal to the time average of the instantaneous frequency. Indeed, the time-average instantaneous frequency appears to bear no simple relation to any feature of the power spectrum (Ville 1948). In the present paper, in order to

highlight essential features of the mechanism, we consider a highly simplified situation.

Experimental Technique

An outline of the experimental technique used to make spectral measurements on ground backscatter echos has been given recently by Earl and Bourne (1975). The essential point is that the signal at a given delay is made up of echos from scatterers in a volume whose depth is of the order of half the pulse length of the transmitter. The location of the volume is fixed by the delay chosen, but it may shift slowly with time if changes in ionospheric properties cause the ray paths and time of group propagation to change with time. A scatterer continues to contribute to the echo at the chosen delay so long as it continues to lie in the volume just described. A spectral analysis may be performed on the echo in the same way as if the echo observed at each cycle of the transmitter repetition cycle was a sample of an underlying continuous process. The repetition from cycle to cycle is important; otherwise a single transmitted pulse of (typically) 1 ms would only allow a spectral resolution of the order of 1 kHz, while spectral detail on a scale of 1 dHz or less is of interest, e.g. the Doppler shifts arising from scatter from moving sea waves is of the order of a few decihertz.

Simple Model

In order to consider the essential features of the experiment, we consider a highly simplified model of the type used by Croft (1969, 1972). We suppose scatterers are located at points x_n along the x axis. Each scatterer gives rise to a contribution of angular frequency ω_0 . Time changes taking place in the ionosphere are supposed to cause the contributing volume described in the previous section to move along the x axis with velocity V . The problem is considered to be essentially one dimensional so that, in a single scatter approximation, the echo signal is given by

$$e(t) = \sum_n \rho_n a(x_n - Vt) \exp\{i(\omega_0 t - \phi_n)\}. \quad (1)$$

Here, ρ_n is the scattering strength of the n th scatterer (initially taken to be identically equal to unity), while ϕ_n is given by

$$\phi_n = 2k_0 x_n + \phi_0. \quad (2)$$

In equation (2), k_0 is the resolved part of the h.f. wave propagation vector. The function $a(-Vt)$ describes the way in which the contribution from a scatterer builds up and eventually dies down again. It can be seen from elementary considerations that the spatial shape of an individual pulse from the transmitter is given by $a(\frac{1}{2}x)$. It should be noticed that, for fixed t , the nonvanishing contributions on the right-hand side of equation (1) do come from scatterers lying in a region whose length is half the pulse length. For convenience in later discussion, we denote the spatial pulse length by p .

Equation (1) may be rewritten as

$$e(t) = \left(\sum_n a(-Vt) * \{\delta(t - x_n V^{-1}) \exp(-2ik_0 Vt)\} \right) \exp\{i(\omega_0 t - \phi_0)\}. \quad (3)$$

If the Fourier transform of this expression exists, it is given by

$$E(\omega) = V^{-1} A^*((\omega - \omega_0)/V) \sum_n \exp(-i\{(\omega - \omega_0)/V + 2k_0\}x_n) \exp(-i\phi_0), \quad (4)$$

where $A(k)$ is the Fourier transform of $a(x)$, and use has been made of the fact that $a(x)$ is real so that $A(-k) = A^*(k)$. From equations (3) or (4) it follows that the power spectrum is given by

$$G(\omega) = V^{-2} |A((\omega - \omega_0)/V)|^2 \lim_{T \rightarrow \infty} T^{-1} \left| \sum_n \exp(-i\{(\omega - \omega_0)/V + 2k_0\}x_n) \right|^2, \quad (5)$$

where the summation extends over n such that $-\frac{1}{2}T < x_n V^{-1} < \frac{1}{2}T$. The function $|A((\omega - \omega_0)/V)|^2$ is symmetrical about ω_0 with a width of the order of $2\pi V p^{-1}$, which is typically very small unless V is very large, or else inhomogeneity in the ionosphere leads to spatial compression of the pulse, so that p is small. The power spectrum can only be nonvanishing at those frequencies for which $|A((\omega - \omega_0)/V)|^2$ is different from zero, while the way in which the contributions from the various scatterers combine depends upon the second factor in the expression (5).

Dependence of Spectrum on Scatterer Distribution

The function $\mathcal{G}(\omega)$ defined by

$$\mathcal{G}(\omega) = \lim_{T \rightarrow \infty} T^{-1} \left| \sum_n \exp(-i\omega\tau_n) \right|^2, \quad (6)$$

with $\tau_n = x_n V^{-1}$ and the range of summation determined as for equation (5), may be recognized as the Fourier transform of the correlation function $\mathcal{R}(\tau)$ of the signal

$$\sum_{n=-\infty}^{\infty} \delta(t - \tau_n).$$

This fact provides some insight. Now, if the positions of the scatterers form a Poisson process of density X^{-1} , that is, they are ‘completely random’, the τ_n form a Poisson process of density VX^{-1} and we then have

$$\mathcal{R}(\tau) = VX^{-1} \delta(\tau) \quad \text{and} \quad \mathcal{G}(\omega) = VX^{-1}. \quad (7)$$

It follows that in this case

$$G(\omega) = (XV)^{-1} |A((\omega - \omega_0)/V)|^2. \quad (8)$$

This is an expression of the familiar proposition that the power of incoherent signals may be added directly. Notice that, if X is decreased, the power in the spectrum is increased. This is to be expected since a reduction in X increases the number of scatterers contributing at a given time.

On the other hand, if the scatterers are distributed periodically with $x_n = nX$ then we have

$$\mathcal{R}(\tau) = VX^{-1} \sum_{n=-\infty}^{\infty} \delta(\tau - nXV^{-1}) \quad \text{and} \quad \mathcal{G}(\omega) = 2\pi VX^{-1} \sum_{n=-\infty}^{\infty} \delta(\omega - 2\pi nVX^{-1}). \quad (9a, b)$$

Either from equation (9b), or using the result (pp. 67–8 of Lighthill 1962)

$$\sum_{n=-\infty}^{\infty} \exp(-in\omega XV^{-1}) = 2\pi VX^{-1} \sum_{n=-\infty}^{\infty} \delta(\omega - 2\pi n VX^{-1}) \quad (10)$$

in equation (4), it follows that

$$G(\omega) = 2\pi XV^{-1} |A((\omega - \omega_0)/V)|^2 \sum_{n=-\infty}^{\infty} \delta(\omega - \omega_0 + 2k_0 V - 2\pi n VX^{-1}). \quad (11)$$

The power spectrum in this case consists of lines at

$$\omega_0 + 2k_0 V, \quad \omega_0 + k_0 V \pm 2\pi m VX^{-1}, \quad \dots$$

The spectrum is thus skewed with respect to ω_0 unless $2k_0 V = 2\pi m VX^{-1}$ holds for some integer m . This latter is just the condition for resonant scattering. The skewing can only be significant on the scale of the width of $|A((\omega - \omega_0)/V)|^2$ if few lines fall within this range, which will be the case if $2\pi VX^{-1}$ is of the order of $2\pi Vp^{-1}$, that is, if about one scatterer falls within a pulse length. The skewing or shift with respect to ω_0 can only be significant if in addition Vp^{-1} , or equivalently VX^{-1} , is large.

Continuous Distribution of Scatterer

The case when the scatter is due to a continuous distribution of irregularity is intuitively more difficult than the discrete case. In order to look at the continuous case we replace the summation in equation (1) by an integration, and write

$$e(t) = \int \rho(x) a(x - Vt) \exp\{i(\omega_0 t - 2k_0 x)\} dx, \quad (12)$$

where the unimportant ϕ_0 has been dropped. Notice that when $t = 0$ we have

$$e(0) = (2\pi)^{-1} \int R(2k_0 - K) A(K) dK, \quad (13)$$

that is, $(2\pi)^{-1}$ times the convolution of the Fourier transforms $R(k)$ and $A(k)$ of $\rho(x)$ and $a(x)$, evaluated at $k = 2k_0$.

Taking the Fourier transform of equation (12) with respect to time leads to

$$E(\omega) = (2\pi)^{-1} \iint R(2k_0 - K) A(K) \exp\{-iKVt\} dK \exp\{-i(\omega - \omega_0)t\} dt, \quad (14)$$

and carrying out the integration with respect to time reduces this equation to

$$E(\omega) = \int R(2k_0 - K) A(K) \delta(\omega - \omega_0 + KV) dK. \quad (15)$$

Finally, using a well-known property of the delta function, we obtain

$$E(\omega) = V^{-1} R(2k_0 + (\omega - \omega_0)/V) A^*((\omega - \omega_0)/V). \quad (16)$$

It should be noted that, if we have $\rho(x) = \sum_n \delta(x - x_n)$, the result (4) is recovered.

From equation (16) it is possible to draw a general conclusion about the possibility of there being a skewing of the spectrum of the echo. Significant skewing on the scale $2\pi Vp^{-1}$ is only possible if $R(k)$, near $k = 2k_0$, changes significantly on a scale $2\pi p^{-1}$. Again, as for the discrete case, the resulting shift in the spectrum is only large if $2\pi Vp^{-1}$ is large.

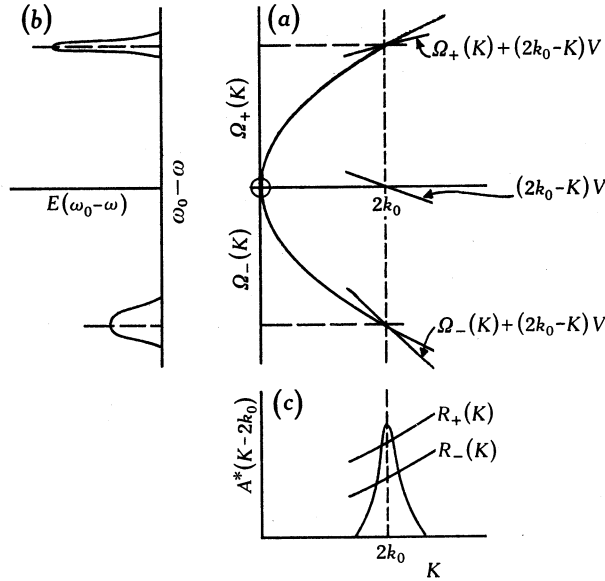


Fig. 1. Spectrum of the echo for scatter from dispersive waves. This is a graphical solution of equations (19) and (20). Part (a) shows a plot of $\Omega(K)$ and part (b) shows a plot of $E(\omega_0 - \omega)$. The mapping from K to $\omega_0 - \omega$ depends upon the value of V , the velocity at which the contributing region moves. Part (c) shows a plot of $A^*(K - 2k_0)$ together with $R_+(K)$ and $R_-(K)$.

Scatter from Dispersive Waves

So far it has been assumed that it is possible to choose coordinates in which the scattering medium appears time stationary. An important case when this cannot be done is when the scatter results from dispersive waves propagating through the medium. In order to extend the simple model to deal with this case, $\rho(x)$ is replaced by $\rho(x, t)$, where

$$\rho(x, t) = (2\pi)^{-1} \int \sum_{+,-} R_{\pm}(K) \exp\{iKx - i\Omega_{\pm}(K)t\} dK, \tag{17}$$

and $\omega = \Omega_{\pm}(K)$ is the dispersion relation for the waves. The two signs allow for the possibility that waves are moving in both directions along the x axis. Frequently we have $\Omega_- = -\Omega_+$, but this need not be the case (e.g. for sea waves superimposed on ocean currents it is violated). Replacing $\rho(x)$ in equation (12) by the right-hand side of (17) and repeating the subsequent analysis quickly leads to

$$E(\omega) = \sum_{+,-} (V - d\Omega_{\pm}/dK)^{-1} R_{\pm}(2k_0 + \{\omega - \omega_0 + \Omega_{\pm}(K)\}/V) A^*(\{\omega - \omega_0 + \Omega_{\pm}(K)\}/V), \tag{18}$$

where K satisfies

$$\omega_0 - \omega = \Omega_{\pm}(K) + (2k_0 - K)V. \quad (19)$$

The analogy with equation (16) is clear from (18).

A more convenient form of the result is obtained if the arguments of the functions are expressed differently using equation (19). Thus we obtain

$$E(\omega) = \sum_{+,-} (V - d\Omega_{\pm}/dK)^{-1} R_{\pm}(K) A^*(K - 2k_0), \quad (20)$$

where again the condition (19) must be satisfied. The implications of equation (20) can be understood from a graphical solution of (19). Fig. 1*a* (the upper right-hand part of Fig. 1) shows a plot of $\Omega(K)$ against K . If $V = 0$, this is also a plot of $\omega_0 - \omega$ against K . Contributions to $E(\omega)$ come from those values of K for which neither $R(k)$ nor $A^*(K - 2k_0)$ vanish (if $A^*(K)$ is vanishingly narrow the only contribution is from $K = 2k_0$). It is thus possible to construct a plot of $E(\omega)$ on the y axis. When V is nonzero the scale of the mapping from K to ω is changed, as indicated in the plot of $E(\omega)$ in Fig. 1*b*. The spectral compression will be large if

$$\partial(\omega - \omega_0)/\partial K |_{K=2k_0} = 0, \quad (21)$$

but from equation (19) this implies

$$\partial\Omega_{\pm}(K)/\partial K |_{K=2k_0} = V. \quad (22)$$

The left-hand side of equation (22) of course represents the group velocity of the scattering waves. The explanation of this result is that the finite volume of the scattering region means that the scatter comes from an effective wave group. The spectrum is narrow if the scattering region follows the wave group, so that its lifetime in the scattering region is large.

Example of Shifts in Spectral Lines

The scatter mechanisms discussed in previous sections can give rise to a shift of the spectral peak if $A^*(k)$ is wide and $R(k)$ is narrow. An example of this type of phenomenon is provided by an acoustic scatter experiment (Dexter 1972) intended as an analogue of the high-frequency sea scatter experiment. The scatter was from capillary waves on the surface of a water tank.

For the case of surface scatter the preceding arguments must be extended to two dimensions. The transforms in equation (20) are then replaced by two-dimensional transforms. The lateral dimension of the contributing region, which is inversely proportional to the corresponding width of $A^*(k)$, is determined largely by the pattern functions of the transmitter and receiver. In the experiment performed by Dexter (1972) the contributing region was in the near field of highly directional transponders, so that the lateral dimension was small. Range gating was not employed, so that the dimension in the direction of propagation was large. In Fig. 2, the region for which $A^*(K - 2k_0)$ is significant is indicated in the K_x, K_y plane.

Dexter (1972) generated capillary waves that were highly collimated in a direction at an angle θ to the illuminating acoustic radiation. This leads to significant $R(K)$ in the region indicated in Fig. 2. The scatter arises from the region of intersection.

Also shown in the figure are lines of constant Ω , that is, the ‘dispersion surfaces’ for the capillary waves. The frequency spectrum of the scatter reaches a peak near a frequency which is shifted from ω_0 by the value of Ω for the dispersion surface that passes through the centre of the region of intersection. Since for capillary waves

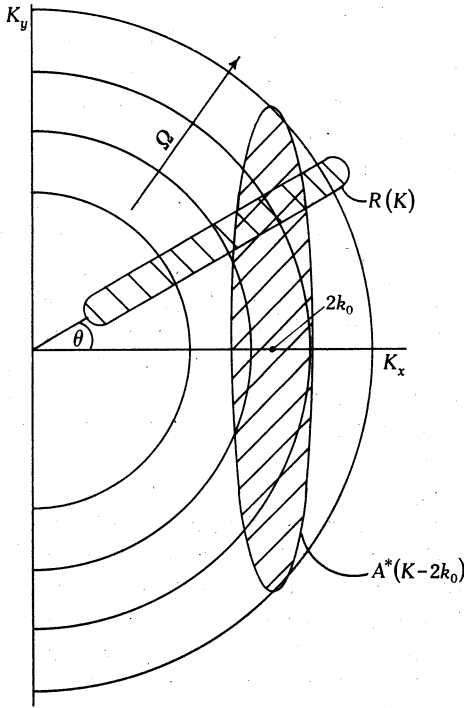


Fig. 2. K plane for scatter from surface waves, indicating how, in a narrow beam system, the Doppler shift of the backscatter echo can vary with the angle θ between the beam and the direction of propagation of well-collimated surface waves.

$\Omega(K)$ is proportional to $|K|^{3/2}$, from Fig. 2 it is clear the dependence on θ of the shift in the spectrum is given by

$$\Omega(2k_0) (\cos \theta)^{-3/2}, \tag{23}$$

to which Dexter’s results conformed very closely. He conjectured that the narrow spectrum of scattering waves may have given rise to this angular dependence. He does not seem to have appreciated the equal importance of the narrow lateral dimension of the contributing region. It is only this that makes possible significant scatter from these waves which do not satisfy a resonance condition.

Discussion and Conclusions

From a study of the simple model discussed in this paper, it can be seen that the effect of movement of the region of space contributing to the scattered echo, which results from time changes in the intervening propagating medium, can be divided into two phenomena. The first effect is to modify the lifetime of the scatterers and hence the maximum possible bandwidth. The second effect, the possible narrowing of the spectrum so that the entire spectrum appears shifted, depends upon the particular nature of the scatterer. However, the bandwidth controlled by the first effect

always remains the limiting factor. While considerable elaboration of the model is necessary in order to deal with realistic ionospheric propagation (as discussed briefly below) some assessment of the likelihood of the predicted effects being observed may be formed.

Since the basic spectral width (in linear not angular frequency) for stationary scatterers is roughly V/p (Hz), a width of 0.5 Hz with $p = 3 \times 10^5$ m (that is, 1 ms) requires a value of $V = 1.5 \times 10^5$ ms⁻¹, while with $p = 3 \times 10^2$ m this width would require a value of $V = 1.5 \times 10^2$ ms⁻¹. Such velocities do not seem likely to occur in normal circumstances. For the case of scatter from waves, with the velocity V of the contributing region zero, the spectral width is of the order of V_g/p . For example, for the case of deep water waves, V_g is half the phase velocity, being of the order of 1 ms⁻¹ for waves giving rise to scatter of high-frequency radio waves. Because of the long distances propagated (of the order of one or two thousand kilometres) the lateral dimension of the contributing region is also large. It does not seem likely that the mechanisms discussed in this paper give rise to significant effects in ionospheric high-frequency backscatter experiments and this conclusion is quite independent of the nature of the scatterer, whether it is periodic or random. (An exception may be experiments performed at short range with highly directional antennas.) However, as has been seen, the effects must be taken into account if scaled models of the ionospheric experiments are to be performed.

The elaboration of the model of this paper to deal with a realistic ionosphere requires attention to a number of points. A ray description of the propagation through the ionosphere, and of the multiple modes that may exist, may be employed but this should ideally allow for the vector nature of the propagation and the weak irregularities in the ionosphere which give rise to loss of correlation in the radiation incident on the scattering region. The correlation length is probably about 1 km, much less than the pulse length in many experiments (Baker 1971). This is important because, in discussing the spectral width associated with the mechanisms considered in this paper, it is the correlation length rather than the pulse length that is important. The scatter may be described in Green's function formulation. Time changes in the ionosphere must also be taken into account and these can give rise to a spectral width that depends upon pulse length. Many of these effects have been included in a numerical simulation by Earl (1975).

Acknowledgments

This paper was written while the author was visiting the Cavendish Laboratory, University of Cambridge, supported by an Alexander von Humboldt Fellowship. It is based in part on work carried out at the University of Düsseldorf supported by an Alexander von Humboldt Fellowship, work at the University of Alberta, Edmonton, Alberta, Canada, supported by the National Research Council of Canada, and work at the University of Melbourne supported by a Commonwealth Post-graduate Award. Useful discussions with Dr I. A. Bourne and Dr G. F. Earl are gratefully acknowledged.

References

- Agy, V. (1969). *J. Geophys. Res.* **74**, 273.
 Baker, P. W. (1971). *IEEE Trans. Antennas Propag.* **AP 19**, 793.

- Barry, G. H., and Wides, P. R. (1962). *J. Geophys. Res.* **67**, 2707.
- Bennett, J. A. (1967). *J. Atmos. Terr. Phys.* **29**, 887.
- Bennett, J. A. (1968). *Aust. J. Phys.* **21**, 259.
- Croft, T. A. (1969). *J. Geophys. Res.* **74**, 3058.
- Croft, T. A. (1972). *Rev. Geophys. Space Phys.* **10**, 73.
- Crombie, D. D. (1955). *Nature (London)* **175**, 681.
- Dexter, P. E. (1972). *Aust. J. Phys.* **25**, 419.
- Earl, G. F., and Bourne, I. A. (1975). Spectral characteristics of H.F. ground backscatter. *J. Atmos. Terr. Phys.* (in press).
- Earl, G. F. (1975). Synthesis of H.F. ground backscatter spectral characteristics. *J. Atmos. Terr. Phys.* (in press).
- Edwards, L. C., and Thome, G. D. (1962). *J. Geophys. Res.* **67**, 2573.
- Lighthill, M. J. (1962). 'Fourier Analysis and Generalized Functions' (Cambridge Univ. Press).
- Ville, J. (1948). *Cables Transm.* **2**, 61.

Manuscript received 2 May 1975

